RESEARCH ARTICLE

Editorial Process: Submission:12/21/2024 Acceptance:05/14/2025

Analysing Differential Alternative Splicing Events and Their Impact on Retinoblastoma Progression Using RNA-seq Metadata

Mohamed Hameed Aslam Assane Rachidou[1,2], Ayyasamy Vanniarajan[3], Usha Kim[4], Bharanidharan Devarajan[1]*

Abstract

Objective: Identify differential alternative splicing (DAS) events and their role in retinoblastoma (RB) progression. **Methods:** We conducted a meta-analysis of RNA sequencing data from 50 RB tumours and 17 normal retinal tissues to identify DAS events and differential expressed genes (DEGs) in RB progression. We performed functional and pathway enrichment analyses, Weighted Gene Co-expression Network Analysis (WGCNA), and protein-protein interaction analysis. **Results:** We identified 6136 DAS events involving 1262 genes and 1787 DEGs. Exon skipping and mutually exclusive exons were the most prevalent DAS events. Functional analyses of DAS events containing genes highlighted involvement in E2F targets, cell cycle, G2M checkpoint, MYC targets and fatty acid metabolism pathways. Notably, numerous DAS events were detected in ENO2. WGCNA identified TFDP1, PCNA, and CCNB1, potentially contributing to RB progression through alternative splicing. Splicing factors ILF2 and HNRNPA1 were highly co-expressed with DAS events containing genes, suggesting their regulatory role in splicing changes during RB progression. **Conclusions:** Our study reveals significant differential alternative splicing events that play a crucial role in the progression of retinoblastoma. Numerous DAS events, DEGs, and functional analyses underscore the complexity of gene regulation in RB. Importantly, DAS events in TFDP1, PCNA, and CCNB1 may play a crucial role, indicating that alternative splicing is a potential avenue for therapeutic intervention in RB.

Keywords: Retinoblastoma- Meta-RNA-seq Data- Alternative Splicing Events- Gene Expression

Asian Pac J Cancer Prev, **26 (5)**, 1781-1792

Introduction

Retinoblastoma (RB) is a rare paediatric eye cancer primarily caused by biallelic inactivation of the RB1 tumour suppressor gene in more than 95% of cases [1]. A small percentage of non-hereditary retinoblastoma (2%) is caused by MYCN gene amplification without RB1 inactivation [2]. In addition to tumour initiation, the progression and characteristics of retinoblastoma involve further alterations, including genetic mutations, epigenetic dysregulation, gene expression changes, and proteomics variations [3]. The most frequently reported alterations include mutations in BCOR and CREBBP, copy number variations (CNVs) involving chromosomes 1q, 2p, 6p, 13q, and 16q [4], altered expression of oncogenes such as *MYCN, E2F3, DEK, KIF14,* and *MDM4,* and chromothripsis [5]. Promoter hypermethylation of the DNA repair gene MLH1, RASSF1A, and MGMT is common in retinoblastoma, leading to its silencing [6]. Moreover, histone modifications cause the upregulation of SYK, which supports tumour progression in retinoblastoma [7]. Proteomic analyses have uncovered critical proteins involved in retinoblastoma progressions, such as B7H3, IGF2BP1, SOX4, and PEDF [8]. Alternative splicing contributes to retinoblastoma progression, which has been less extensively studied in this context [9].

A comprehensive analysis of RB1 mutations has shown that 4-15% occur in splice sites [10], suggesting that altered splicing affects the RB1 gene and initiates RB [11]. Several studies have documented exon-skipping events in the RB1, MDM4, and Dab1 genes in RB patients[12]. However, a complete profile of alternative splicing events and their role in RB tumour progression remains elusive.

RNA-seq transcriptomic data has been widely used to identify alternative splicing events in cancer progression. Yang et al. [13] used RB transcriptome data from a single study to detect differential alternative splicing (DAS)

*[1]Department of Bioinformatics, Aravind Medical Research Foundation, Madurai, India. [2]Department of Bioinformatics, Alagappa University, karaikudi, India. [3]Department of Molecular Genetics, Aravind Medical Research Foundation, Madurai, India. [4]Department of Orbit, Oculoplasty and Oncology, Aravind Eye Hospital, Madurai, India. *For Correspondence: bharani@aravind.org*

events in retinoblastoma. They identified exon skipping and mutually exclusive exons as the most predominant DAS events, mostly enriched in E2F family transcription factors, the visual sense gene ABCA4, and the splicing factor DAZAP1, suggesting their role in RB progression. However, since the SRA database (https://www.ncbi.nlm.nih.gov/sra) contains several studies with RNA-seq transcriptomics data from RB patients, a meta-analysis of RB will provide comprehensive profiling and more true-positive alternative splicing events in RB progression. Thus, in this study, we performed a comprehensive, integrated meta-analysis of gene expression and alternative splicing events by comparing RB with normal retinal tissue, aiming to uncover dysregulated pathways, transcription factors, and splicing factors with aberrant splicing events leading to RB progression. Our findings provide novel insights into the molecular mechanisms underlying RB progression and highlight potential therapeutic targets. They also pave the way for future studies in this field, offering a beacon of hope for improved understanding and treatment of RB.

Materials and Methods

RNAseq data of retinoblastoma tumour tissue was collected from the Sequence Read Archive (SRA) database (https://www.ncbi.nlm.nih.gov/sra) from their inception up to September 7, 2023. After manual curation of sample details, the SRA files of 50 RB tissues and 17 retinal tissues were obtained by removing the fetal retina and para-tumour from the following retinoblastoma project with accession PRJNA728725, PRJNA343264, PRJNA752257, PRJNA693838, PRJNA494224, PRJNA436090, PRJNA658590, PRJNA517916 (Table 1). The selected sample data were downloaded as SRA files and converted to FASTQ format using fastq-dump from the SRA toolkit (https://github.com/ncbi/sra-tools). We removed the low-quality reads and adapters using the fastp tool [14]. Further, the cleaned raw reads were indexed and aligned to the ensemble human reference genome (GRCh38 release-104) fasta file with its annotation GTF file by STAR (v2.7.9a) [15]. In addition, the parameter options were changed accordingly based on the type of libraries (stranded or unstranded). Further, we quantified the aligned reads as raw counts using featureCounts (v2.0.3) [16]. The phenotype quantile technique normalised the raw counts. Furthermore, the early merging technique was adopted to conduct a gene set test in the meta-analysis of transcriptome data. Principal Component Analysis (PCA) was performed to assess the batch effect, and outliers were removed, as illustrated in Supplementary Figure S1.

Differential Genes Expression Analysis

The normalised count was used by the R edgeR(v3.30) [17] package to conduct the differential expression analysis. The dispersion was estimated and fitted to a negative binomial generalised log-linear model by edgeR functions. QL (Quasi-likelihood) F-Test statistics and log2 fold change were used to evaluate the statistical significance (FDR<0.05, logCPM>0.5 and log2 fold change > ±2).

Differential Alternative Splicing Analysis

rMATS [18] was used to screen differential alternative splicing events across all samples. The ensemble human reference (GRCh38 release 104) annotation GTF file and aligned bam files were given as input for rMATS with the default parameters. We selected Differential Alternative Splicing (DAS) events with FDR<0.05. The deltaPSI value was computed by subtracting the average PSI (IncLevel) value of the control group(retina) from the average PSI value of the tumour group (RB), expressed as follows: deltaPSI = Average (Tumour_PSI) - Average (Control_PSI).

Functional and pathway enrichment analysis of DAS and DEG

The cluster Profiler [19] R package(version 4.0) was used to perform gene functional enrichment analysis of the differentially expressed genes (DEGs) and genes with differential alternative splicing (DAS). The analysis included Gene Ontology (GO), Kyoto Encyclopedia of Genes and Genomes (KEGG) and hallmark signature datasets from Molecular Signature (MsigDB). The DEGs and DAS events were first converted from Ensembl IDs to gene symbols and Entrez IDs using the clusterProfiler annotation package. The Entrez IDs were then used as input for the enrichment analysis. Enriched pathways and gene sets were identified based on a false discovery

Table 1. RNAseq Data were Collected from Projects in Public Repositories. The table lists the project accession IDs, the number of tumour samples, control retina samples, fetal retina samples, and para-tumour samples, along with the reference for each project.

Project accession ID	Tumour	Control Retina	Fetal Retina	Para-tumour	Reference
PRJNA728725	21		3		Norrie JL et al., 2021
PRJNA343264	1		8		Aldiri I et al., 2017
PRJNA752257	5	5			not available till (7-9-2023)
PRJNA693838	5	3			not available till (7-9-2023)
PRJNA494224	1				Saengwimol D et al.,2018
PRJNA436090	3			3	Ni H et al., 2020
PRJNA658590	7	3			Amit Chatterjee et al., 2021
PRJNA517916	7	3			Rajasekaran S et al., 2019
Total	50	17	11	3	

rate (FDR) cutoff of adjusted p-value < 0.05. From the results of enriched genes and pathways from the hallmark signature of the MsigDB database, a functional interaction network was constructed and visualised using a Cytoscope 3.1 [20].

Weighted Gene Co-expression Network Analysis

We conducted a Weighted Gene Co-expression Network Analysis (WGCNA) [21] on the transcripts of genes exhibiting differential alternative splicing using gene-level summarised transcript expression data. Our analysis employed stepwise module detection methods, starting with constructing a sample tree through hierarchical clustering to identify outliers. Next, we determined the soft threshold beta for scale-free topology using the mean connectivity and R^2 correlation coefficient from the pickSoftThreshold() function. Subsequently, the weighted adjacency matrix and dissimilarity matrix were established using the adjacency () and TOMdist() functions. We then calculated RB tumour tissue co-expressions with DAS, treating them as weights for the analysis.

Further, we computed the Pearson correlation matrix for gene pairs and employed the Dynamic Tree Cut algorithm to group genes into modules, using a merging threshold function of 0.25. Subsequently, we identified modules associated with traits. The traits' expression matrix was crafted by integrating the expressions of differential splicing factors genes, RB tumour tissue, and control retina tissue. Following that, we calculated gene significance and module membership to discern the relationship between genes and traits and the importance of each module. Lastly, we pinpointed a highly correlated module from the module-trait relationship, selecting hub genes with high gene significance (correlation between gene and trait) > 0.2 and Module Membership (correlation of the module eigengene and the gene expression profiles) > 0.8 through intramodular analysis.

Comprehensive Protein-Protein interaction analysis

Protein-protein interaction (PPI) information of significant module genes identified from WGCNA modules of DAS and splicing factor was obtained from the Search Tool for the Retrieval of Interacting Genes (STRING) database (https://string-db.org/). The PPI network was produced using Cytoscape software, and the degree of nodes was calculated using the Cytohuba program in Cytoscape software.

Identification of the hub genes from WGCNA

We identified the candidate genes from the significant module extracted through Weighted Gene Co-expression Network Analysis (WGCNA). Subsequently, we performed a sub-network analysis to identify hub genes. VarEelct [22] was then employed to analyse the relationship between the identified key genes and retinoblastoma.

Results

Identification of differential alternative splicing events in retinoblastoma

This comprehensive analysis identified 6136 significant differential alternative splicing events involving 1262 distinct genes (Table 2). The most common event type observed was Mutually Exclusive Exons (MXE), accounting for 41.6% of occurrences, followed closely by Skipped Exons (SE) at 35.8%. Retained Intron (RI) accounted for 8.4% of events, while Alternative 3' splicing site (A3SS) and Alternative 5' splicing site (A5SS) represented 8.1% and 6.1% respectively (Figure 1B). In terms of the distribution of DAS genes, SE (734) had a higher count than MXE (573) (Figure 1A). Noteworthy genes, including *PCBP4, MYL6, HMGN1, GUK1,*

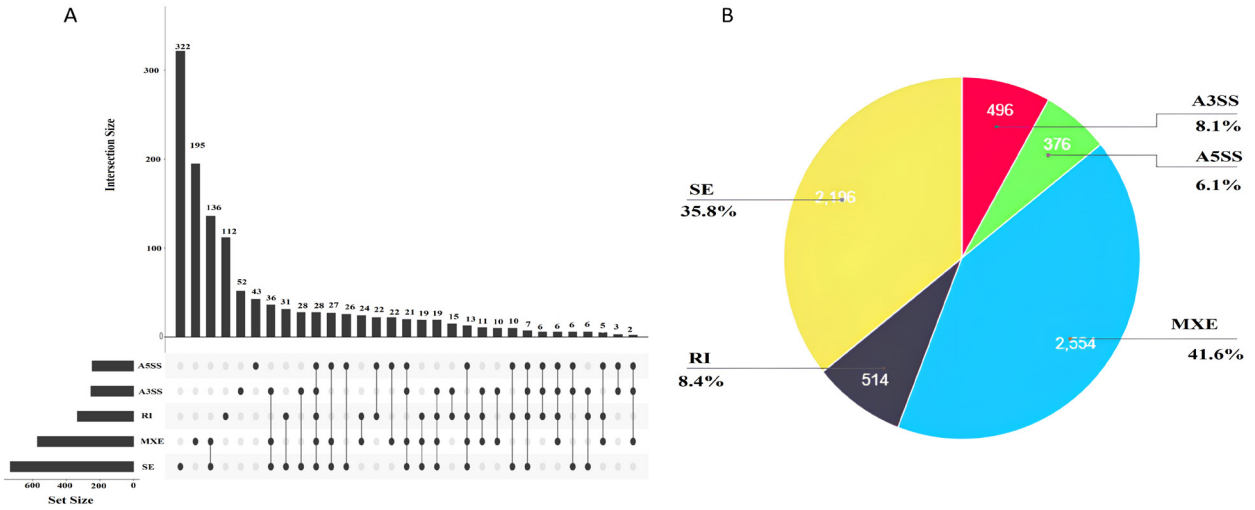

Figure 1. Distribution of Differentially Alternatively Spliced (DAS) Events and Genes in the Analysed Dataset. (A) An upset plot depicts the number of genes undergoing each type of alternative splicing (AS) event. The left side strips show the number of genes affected by each AS type, while the dots in the matrix represent the AS types included in each subset. The histogram on top displays the number of genes in each subgroup. (B) Pie chart illustrating the distribution of AS events. The chart segments represent the proportion of each AS event type: RI (retained intron), A5SS (alternative 5' splice site), A3SS (alternative 3' splice site), MXE (mutually exclusive exons), and SE (skipped exon)

Table 2. The List of Significant DAS Events and Corresponding Genes for Each of the Five Main Types of Alternative Splicing: alternative 3' splice site (A3SS), alternative 5' splice site (A5SS), mutually exclusive exons (MXE), retained intron (RI), and skipped exon (SE).

Events Type	Significant Differential AS Events	DAS genes for each event
A3SS	496	255
A5SS	376	246
MXE	2554	573
RI	514	334
SE	2196	734
Total	6136	2143

ENO2, HNRNPC, PKM, HNRNPA1, RPLP0, and *PTMS* (in descending order), exhibited a high prevalence of differential alternative splicing events (Supplementary Table S1, S2).

All the five types of alternative splicing events were noted in the following 27 DAS genes, including *BAG6, CAMK2B, CKB, CUTA, EEF1D, ENO2, FLOT1, GNB3, HMGN1, HMGN2, HNRNPA1, HNRNPC, HNRNPH1, MYL6, NT5DC2, PCBP2, PCBP4, PRRC2A, PTMA, PTMS, RACK1, RPS18, RPS24, SNHG1, SNHG29, SNHG5*, and *YIPF3* (Supplementary Table S2). Notably, the gene *PTMS* exhibited the highest count in A3SS and RI events, while *PCBP4* accounted for the largest numbers in MXE and SE events, and *MYL6* accounted for most A5SS events. This intricate characterisation enhances our understanding of retinoblastoma's differential alternative splicing landscape.

Differential gene expression analysis in retinoblastoma

Differential gene expression analysis compared the transcriptomic profiles of retinoblastoma (RB) and normal retinal tissue. A total of 1787 DEGs were identified, with 1140 genes showing upregulation and 647 genes exhibiting downregulation (Figure 2). Among the most significantly upregulated genes were *MMP12, SP9*, and *DNMT3L*, while *OVCH2, PIP*, and *PDE6A* were found to be among the most downregulated genes (Supplementary Table S3).

Functional and pathway enrichment analysis of genes with DAS in retinoblastoma

The functional enrichment analysis of 1262 DAS genes, which included Gene Ontology (GO), the Kyoto Encyclopedia of Genes and Genomes (KEGG), and the Hallmark gene signature set from the Molecular Signature Database (MsigDB), revealed pathways pertinent to tumour progression (see Figure 3 and Supplementary Table S4). Among these, 536 GO terms showed significant enrichment (P.adj < 0.05), categorised into Biological Process (334 terms), Cellular Component (134 terms), and Molecular Function (67 terms). The top ten enriched GO terms were primarily associated with RNA splicing (including RNA splicing, RNA splicing via transesterification reactions with bulged adenosine as

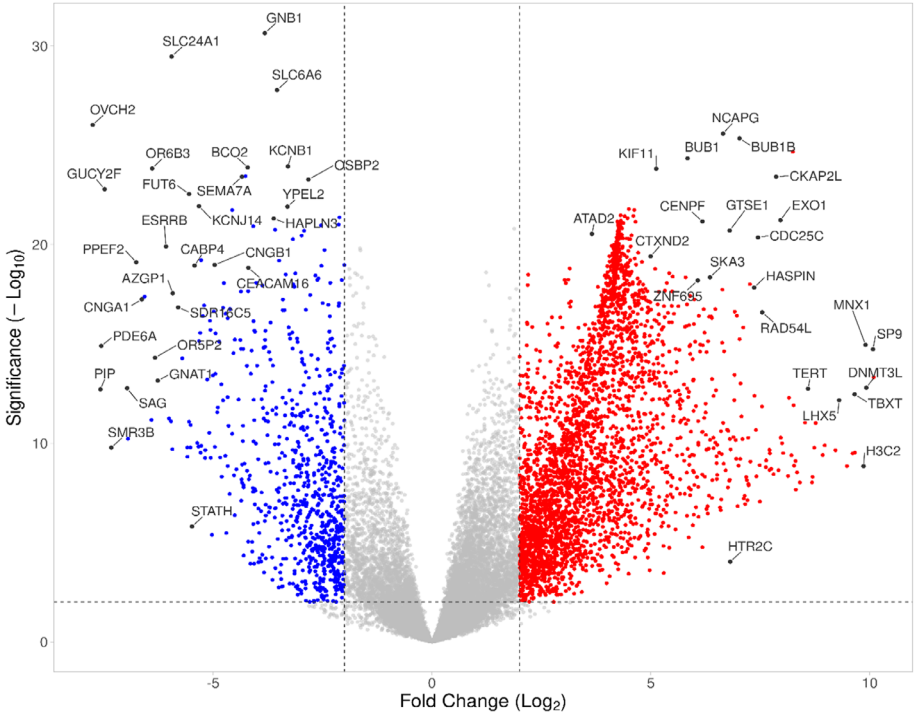

Figure 2. Volcano Plot Showing Differentially Expressed Genes (DEGs) between Control Retina and Retinoblastoma (RB) Tumour Samples. The x-axis represents the log2 fold change in gene expression, while the y-axis shows the negative log10 of the p-value. Each dot represents an individual gene. The dashed horizontal line indicates the statistical significance threshold of $p < 0.05$, corresponding to -log10(p-value) = 1.3. The two vertical dashed lines represent a log2 fold change cutoff of ±2. Blue dots on the left side denote downregulated DEGs, while red dots on the right side represent upregulated DEGs. The top 50 most significantly differentially expressed genes are labelled on the plot.

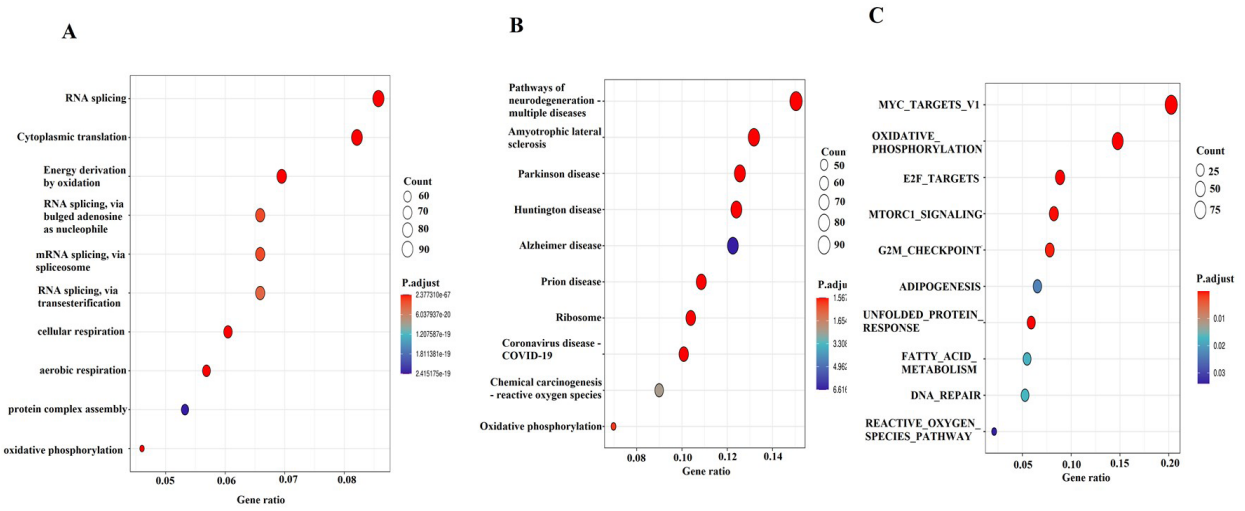

Figure 3. Bubble Plots Showing Functional Enrichment Analysis of Differentially Alternatively Spliced (DAS) Genes. (A) Gene Ontology (GO) terms enriched among DAS genes. (B) Kyoto Encyclopedia of Genes and Genomes (KEGG) pathways enriched among DAS genes. (C) Molecular Signatures Database (MSigDB) pathways enriched among DAS genes. In each plot, the x-axis represents the gene ratio, which is the proportion of DAS genes associated with each term or pathway. The size of the bubbles indicates the number of DAS genes enriched in each term or pathway, while the colour represents the statistical significance of the enrichment (adjusted p-value) according to the colour scale provided.Terms or pathways with smaller adjusted p-values (darker colours) are considered more significantly enriched.

nucleophile, mRNA splicing via spliceosome, and RNA splicing via transesterification reactions), translation (cytoplasmic translation), and energy production (energy derivation by oxidation of organic compounds, cellular respiration, aerobic respiration, and oxidative phosphorylation). The prominence of RNA splicing-related terms, particularly those involving transesterification and spliceosome machinery, suggests that these genes may regulate splicing events. The enrichment of mRNA splicing terms further corroborates this. Moreover, the enrichment of terms related to cellular respiration, aerobic respiration, and oxidative phosphorylation indicates that these DAS genes might also enhance cellular energy production through oxygen-dependent pathways. This could support splicing activity or other cellular processes regulated by these alternatively spliced transcripts.

Furthermore, 45 KEGG pathways demonstrated significant enrichment (P.adj < 0.05) with the DAS genes. The top ten enriched pathways in KEGG were associated with Neurodegenerative Diseases, including pathways of neurodegeneration involving multiple diseases, Amyotrophic lateral sclerosis, Parkinson's

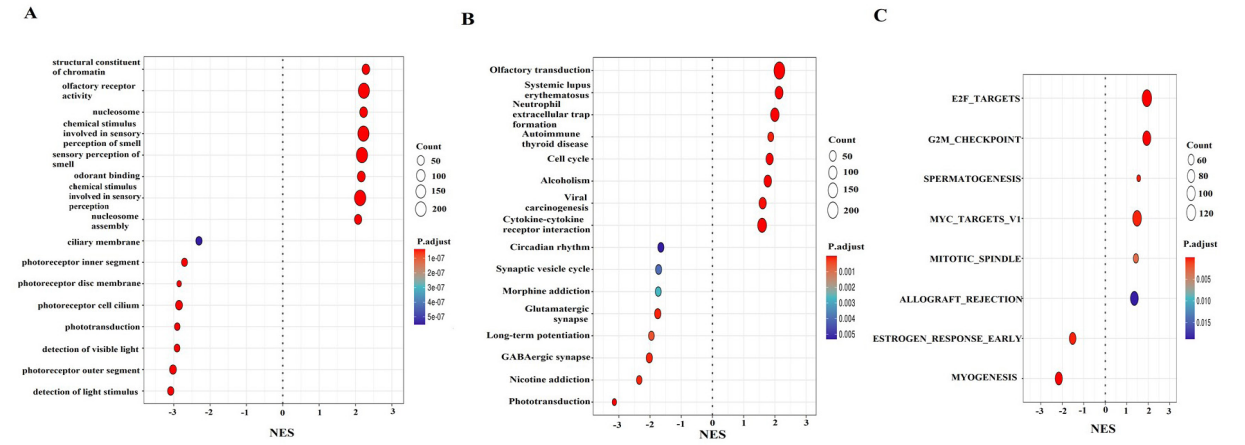

Figure 4. Bubble Plots Depicting Gene Set Enrichment Analysis (GSEA) Results for Differentially Expressed Genes (DEGs). (A) Gene Ontology (GO) terms enriched among DEGs. (B) Kyoto Encyclopedia of Genes and Genomes (KEGG) pathways enriched among DEGs. (C) Molecular Signatures Database (MSigDB) pathways enriched among DEGs. The x-axis represents the normalized enrichment score (NES), which reflects the degree to which a gene set is overrepresented at the top or bottom of a ranked list of genes. A positive NES indicates gene set enrichment at the top of the ranked list (upregulated genes). In contrast, a negative NES indicates gene set enrichment at the bottom of the ranked list (downregulated genes). The size of the bubbles represents the number of DEGs enriched in each term or pathway, while the colour indicates the statistical significance of the enrichment (adjusted p-value) according to the colour scale provided. Terms or pathways with smaller adjusted p-values (darker colours) are considered more significantly enriched.

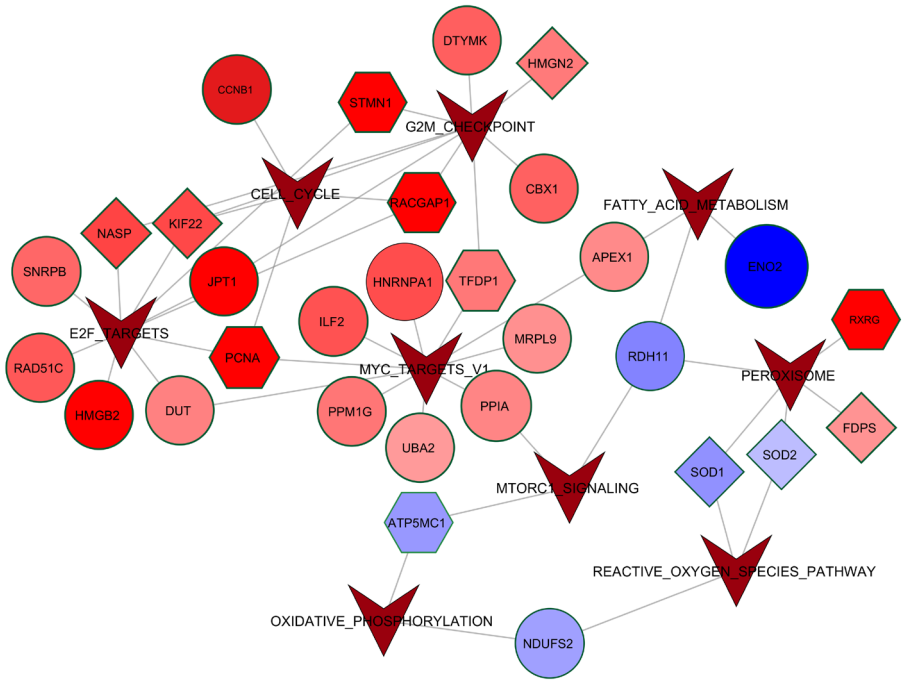

Figure 5. Functional Network Highlighting Significant DAS Genes and their Pathways. The nodes represent genes and pathways, while the edges denote their associations. Gene nodes are categorised based on their DAS status: circles indicate downregulated DAS genes, hexagons represent upregulated DAS genes, and diamonds signify non-significant DAS genes. The colour gradient of the gene nodes reflects their expression levels, ranging from red (highly upregulated) to blue (highly downregulated). Pathway nodes are depicted as downward triangles.

disease, Huntington's disease, Prion disease, and Alzheimer's disease. Additionally, pathways related to Cellular Processes, such as Ribosome and Oxidative phosphorylation, and Disease Pathogenesis and Response, including Coronavirus disease (COVID-19) and Chemical carcinogenesis involving reactive oxygen species, were highlighted. The enrichment of these KEGG pathways, particularly those related to neurodegenerative diseases and immune-related pathways, suggests potential molecular connections between retinoblastoma and neurodegeneration, as well as immune dysregulation in tumour pathogenesis.

We identified significant enrichment in ten Hallmark gene sets related to Cellular Stress Responses and Signaling (Unfolded Protein Response and Reactive Oxygen Species), Metabolism (Fatty Acid Metabolism,

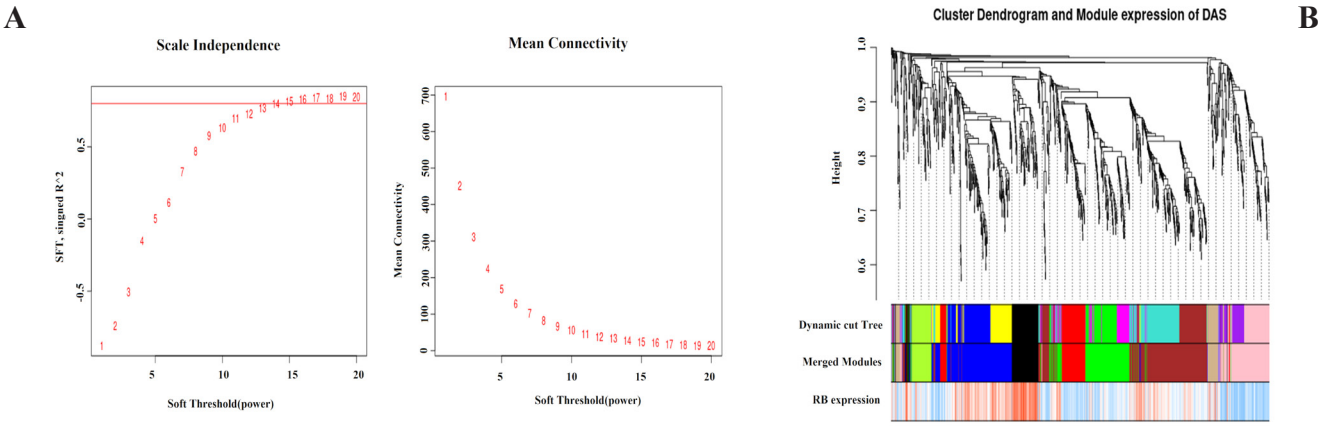

Figure 6. Construction of a Weighted Gene Co-Expression Network Analysis (WGCNA) Using Differentially Alternatively Spliced (DAS) Genes. (A) Analysis of network topology for various soft-thresholding powers (β). The left panel displays the scale-free fit index (y-axis) as a function of the soft-thresholding power (x-axis). The right panel shows the mean connectivity (degree, y-axis) as a function of the soft-thresholding power (x-axis). The red line in the left panel represents the correlation coefficient threshold of 0.8. The soft-thresholding power of 19, where the scale-free topology fit index reaches 0.8, was chosen for subsequent analysis. (B) The dendrogram illustrates the hierarchical clustering of genes based on their co-expression patterns. The y-axis represents the height or distance between clusters, while the x-axis shows the genes grouped into distinct modules. The dendrogram branches are colour-coded to represent different co-expression modules. Each colour corresponds to a group of genes with highly correlated expression patterns across samples. The black module highly correlated with gene expression in RB.

mTOR Signaling, Peroxisomes), and Cell Cycle Regulation (E2F Targets, G2M Checkpoint, MYC Targets) with a P.adj < 0.05. These findings were initially visualised in a bubble plot (Figure 3 and Supplementary Table S4) and later transformed into a network format using Cytoscape, incorporating additional attributes such as DAS and DEG gene expression levels and the count of alternative splicing events (Figure 5). Based on betweenness centrality by degree, pathways such as MYC target genes, oxidative phosphorylation, E2F targets, and G2M checkpoint were predominantly dysregulated by differentially alternative spliced genes. Among these, MYC Target genes showed decreased alternative splicing events and upregulated expression compared to the control retina. The MYC family of transcription factors, known as proto-oncogenes, are implicated in regulating alternative splicing [23]. The Hallmark MYC Targets v1 gene set includes genes often upregulated in cancer cells where MYC is overactive [24]. A recent study by Phillips et al. [25] suggested that MYC targets tend to downregulate with increased splicing activity due to the introduction of stop codons. Nodes common between E2F targets and G2M checkpoint were upregulated in gene expression and showed increased alternative splicing in RB tumours. Another enriched molecular signature was the Fatty Acid Metabolism pathway. Notably, ENO2, a glycolysis enzyme, exhibited more alternative splicing events and decreased differential splicing and gene expression in tumours compared to the retina. This gene is implicated in cancer progression [26].

Functional and pathway enrichment analysis of DEGs in retinoblastoma

The functional enrichment and pathway analysis were performed on the 1787 genes identified from the differentially expressed genes (DEG). As shown in Figure 4 and Supplementary Table S4, a total of 377 Gene Ontology (GO) terms showed significant enrichment (P.adj < 0.05), distributed across Biological Process (277 terms), Cellular Components (57 terms), and Molecular Function (43 terms). Additionally, 47 Kyoto Encyclopaedia of Genes and Genomes (KEGG) pathways exhibited significant enrichment (P.adj < 0.05) with DEG genes. Notably, eight Hallmark gene sets displayed significant enrichment (P < 0.05) and are linked to cell Cycle Regulation (E2F Targets, G2M Checkpoint, Mitotic Spindle), Muscle Development and Function (Myogenesis), Reproductive Processes (Spermatogenesis, Estrogen Response Early), Oncogenic Pathways (MYC Targets V1) and Immune Response (Allograft Rejection). The bubble plot (Figure 4 and Supplementary Table S4) shows the functional enrichment analysis of DEGs. The dysregulation in the cell cycle pathway is linked to the progression of retinoblastoma (RB) cancer [27]. Pathways related to the functional loss of the retina were highly enriched with the most DEGs in suppressed pathways. The impairment of retinal function or vision in retinoblastoma is critical to RB progression, as highlighted by Warda et al. [28].

Identifying hub genes with differential alternative splicing (DAS) using weighted gene co-expression network analysis (WGCNA) in retinoblastoma

The construction of the Weighted Gene Co-expression Network Analysis (WGCNA) network aimed to identify co-expression modules by utilising the expression profiles of genes exhibiting DAS between the control retina and RB tumour samples as described in methods. The soft threshold power was calculated as 19 to establish a scale-free network, corresponding to the correlation coefficient square value and mean connectivity (Figure 6A). Modules sharing high similarities were merged, resulting in the identification of nine distinct gene modules. RB tumour expression served as the weight for our analysis (Figure 6B). We selected the black module from the modules that exhibited a high correlation with RB tumour expression (Supplementary Figure S2 A). We then identified 42 significant candidate genes that have the potential to act as hub genes related to RB tumours within the black module (Supplementary Figure S2 B).

We constructed the sub-network using black module genes and pathways from *GO, KEGG*, and MsigDB (Supplementary Figure S3). We identified eight hub genes: *PCNA, TFDP1, KIF22, CCNB1, NASP, APEX1, DUT,* and *RACGAP1* by analysing high betweenness and closeness centrality scores through degree measures. The VarElect tool analysed the correlation between these hub genes and retinoblastoma. Based on the VarElect scores, we identified *TFDP1, PCNA*, and *CCNB1* genes, suggesting that DAS events of these genes play an important role in retinoblastoma progression.

Identifications of splicing factors and their associated genes involved in retinoblastoma

Wang et al. [29] identified 118 DNA- and RNA-binding protein (DRBP) genes as splicing factors, out of which seven genes *LIN28, RBM15, ILF2, DDX1, YBX3, HNRNPA1*, and *MBNL2* were found to be differentially expressed between control retina samples and RB tumour samples, indicating their role as differential splicing factors. Module-trait relationship analysis reveals differential splicing factors ILF2 and HNRNPA1 were highly co-expressed with the black module in DAS (Supplementary Figure S2 A) associated with RB tumour expression. The Protein-Protein interaction (PPI) network was constructed to infer interaction between the IFL2, HNRNPA1 and the DAS genes from the black module (Supplementary Figure S4). The following DAS genes, *YBX1, KHDRBS1, SRSF10, VPS72, SNRPB, HNRNPD, MRPL9, HSP90AB1, PPIA, MAZ, SQSTMT, TRIM28, RBMX, PTMA, UBA2, PFDN6 ,SRSF1, NONO, SRSF7,* and *HNRNPA3* showed potential interaction with splicing factor IFL2 and HNRNPA1. Therefore, ILF2 and HNRNPA1 may regulate the alternative splicing events in the above DAS genes during retinoblastoma progression.

Discussion

Alternative splicing has extensively been studied for its role in cancer progression. However, it is not studied exclusively in retinoblastoma progression beyond the

RB1 gene using RNA-seq data. In this study, We adopted a comprehensive meta-analysis approach, pooling data from eight studies and analysing 70 samples of RNA sequencing data from retinoblastoma compared to normal retinal tissues. We show that MXE (41.6 %) accounts for the most alternative events, followed by SE (38.8%). Similarly, Yang et al., [13] have shown that MXE and SE are predominant events in RB using single RNA-seq data. Also, it was observed that MXE events were more prevalent in multiple myeloma, making up 44.3%, followed by SE (36.2%), suggesting that MXE and SE are predominant in RB progression.

DAS and DEG functional enrichment analyses commonly identified cell cycle regulation pathways, such as E2F targets and G2M checkpoint, with upregulated gene expression and predominantly increased alternative splicing events in RB tumours (Figure 4 & 5). Additionally, both analyses highlighted the involvement of the MYC target gene pathway, although DAS genes showed mostly decreased alternative splicing events and upregulated expression, while DEGs were enriched in the MYC targets V1 gene set. Pathways such as neurodegenerative diseases (Amyotrophic lateral sclerosis, Parkinson's disease, Huntington's disease, Prion disease, and Alzheimer's disease), cellular processes (ribosome and oxidative phosphorylation), disease pathogenesis and response (COVID-19 and chemical carcinogenesis), cellular stress responses (unfolded protein response and reactive oxygen species), and metabolism (fatty acid metabolism), mTOR signalling, and peroxisomes were uniquely enriched in DAS analysis [30–33] Among these DAS genes, *ATP5MC1, NDUFS2, RDH11, RPS14, SOD1, SOD2* were enriched in all the pathways. DAS genes uniquely found in these pathways are given supplementary Table S4. In contrast, DEGs were uniquely enriched in pathways associated with muscle development and function (myogenesis), reproductive processes (spermatogenesis and early estrogen response), oncogenic pathways, and immune responses (allograft rejection) [34–40]. Among these DEG genes, *CCNA1, DCC, HDAC2, IGF1, ITGA2B, MAPK12, PRKCB, RAC2*, and *TNNC1* were enriched in all the pathways. DEG genes uniquely found in these pathways are given in supplementary Table S3. These findings suggest that while DAS and DEGs contribute to cell cycle dysregulation in retinoblastoma, they also have distinct roles in various biological processes and pathways related to tumour progression and cellular functions.

Functional enrichment of DAS genes showed Fatty acid metabolism as one of the major pathways in which ENO2 (Enolase2) had the most DAS events. ENO2, a key glycolytic enzyme associated with lipid biosynthesis and energy homeostasis in cancer, has been previously linked to these processes [41, 42]. Altered splicing of ENO2 may enhance metabolic adaptability in RB by increasing glycolytic flux, which can elevate intermediates for fatty acid synthesis and support rapid tumour growth [43]. The cancer cells depend on lipid metabolism for membrane biosynthesis and survival under hypoxic conditions [44, 45], reinforcing the role of ENO2 as a metabolic regulator in RB. These findings suggest that targeting ENO2 splicing variants and their associated metabolic effects could offer novel therapeutic strategies for RB treatment.

Additionally, This study identified eight hub genes *PCNA, TFDP1, KIF22, CCNB1, NASP, APEX1, DUT,* and *RACGAP1* through WGCNA analysis. These hub genes are significantly enriched in several biological processes, including the cell cycle, G2M checkpoint, E2F targets, DNA repair and maintenance, chromatin and nucleosome organisation, and fatty acid metabolism [46–48] (Supplementary Figure S3). Among these, *PCNA*, *TFDP1*, and *CCNB1* were highlighted as key genes due to their high varelect scores, indicating a strong association with retinoblastoma. The predicted alternative splicing events (ASE) for these hub genes are as follows: *TFDP1* has 1 A3SS, 4 MXE, and 3 SE events; *PCNA* exhibits 1 A5SS and 11 MXE events; and *CCNB1* shows 1 SE event. *TFDP1* (Transcription Factor Dp-1) is a dimerisation partner for the E2F family of transcription factors, which are essential regulators of cell cycle progression and are often deregulated in various cancers [49]. Alternative splicing of *TFDP1* may lead to the formation of different isoforms with distinct functions, potentially contributing to the dysregulation of cell cycle control [50]. *TFDP1* was differentially expressed in retinoblastoma compared to the normal retina and altered *TFDP1* splicing might affect its transcriptional role [51]. Similar to its role in retinoblastoma, *TFDP1* has been found to be differentially expressed in glioblastoma compared to normal brain tissue [52]. *PCNA* (Proliferating Cell Nuclear Antigen) is a key player in DNA replication and repair, and its expression is often altered in cancer cells [53]. Alternative splicing of *PCNA* may produce variants with different cellular localisation and functions, possibly promoting cell proliferation and genomic instability [54]. The retinoblastoma protein (RB) disrupts *PCNA* chromatin tethering in S-phase cells, inhibiting DNA replication [55]. The changes in *PCNA* alternative splicing may impact RB's regulation. *CCNB1* (Cyclin B1) is a crucial regulator of the G2/M transition in the cell cycle, and its aberrant expression has been linked to various cancers [56]. Alternative splicing of *CCNB1* may generate isoforms with altered stability or activity, potentially contributing to the deregulation of cell cycle progression [57]. Given the involvement of these key genes in critical cellular processes and their dysregulation in RB and other cancers, we speculate that alternative splicing of *TFDP1*, *PCNA*, and *CCNB1* may contribute to the development and progression of retinoblastoma, warranting further investigation into their specific roles and potential as therapeutic targets.

The module-trait relationship analysis and protein-protein interaction (PPI) network provide essential insights into the role of alternative splicing and splicing factors in retinoblastoma (RB) tumour progression. The results show that the splicing factors ILF2 and HNRNPA1 are highly co-expressed with a set of differentially alternatively spliced (DAS) genes in the black module associated with RB tumour expression (Supplementary Figure S2 and Figure S3). ILF2 (interleukin enhancer binding factor 2) and HNRNPA1 (heterogeneous nuclear ribonucleoprotein A1) are known to regulate alternative splicing of pre-mRNA [58, 59]. The high co-expression

suggests these splicing factors may drive RB's observed alternative splicing changes. The PPI network further reveals that ILF2 and HNRNPA1 potentially interact with 20 specific DAS genes in the black module, including *YBX1, KHDRBS1, SRSF10, SRSF1, SRSF7* and others (Supplementary Figure S4). Many of these genes are splicing factors or regulators, such as the SR proteins SRSF1, SRSF7, and SRSF10, which are crucial for regulating the alternative splicing of numerous genes [60]. YBX1 modulates alternative splicing by regulating splicing factor activities [61]. Therefore, the interaction of ILF2 and HNRNPA1 with these DAS genes suggests they regulate the splicing changes directly or indirectly by modulating the activity of other splicing factors during RB progression. The additional DAS genes interacting with ILF2 and HNRNPA1, despite not being splicing factors themselves, have varied functions in transcription (TRIM28, MAZ), translation (MRPL9), protein folding (HSP90AB1, PFDN6), and protein degradation (SQSTM1, UBA2), with their alternative splicing potentially influencing these crucial cellular processes to promote RB tumour growth [62–66].

In summary, functional analyses of DAS events containing genes highlighted involvement in E2F targets, cell cycle, G2M checkpoint, MYC targets and fatty acid metabolism. Notably, numerous DAS events were detected in ENO2. WGCNA identified *TFDP1*, *PCNA*, and *CCNB1*, potentially contributing to RB progression through alternative splicing. Splicing factors ILF2 and HNRNPA1 were highly co-expressed with DAS events containing genes, suggesting their regulatory role in splicing changes during RB progression. This reveals a coordinated alternative splicing program where specific splicing regulators modify cancer-associated pathways through transcript diversification, creating molecular trajectories that accelerate RB progression through metabolic reprogramming, immune evasion, and enhanced proliferative signaling. Future research directions should prioritize experimental validation of the identified splicing events and interactions, coupled with mechanistic studies to unravel the molecular pathways governing these processes. Additionally, systematic investigation of the therapeutic potential of targeting these splicing factors and hub genes could yield critical insights for developing retinoblastoma treatment strategies.

In conclusion, our comprehensive meta-analysis of RNA sequencing data from retinoblastoma and normal retinal tissues has revealed significant insights into the role of alternative splicing in retinoblastoma progression beyond RB1 mutation. We identified 1787 differentially expressed genes (DEGs) and 6136 differential alternative splicing (DAS) events, with exon skipping and mutually exclusive exons being the most prevalent. Functional and pathway enrichment analyses highlighted the involvement of E2F targets, cell cycle, G2M checkpoint, MYC targets and fatty acid metabolism in retinoblastoma. Key genes such as *ENO2, CCNB1, PCNA*, and *TFDP1* were identified as potential contributors to RB progression through alternative splicing. Additionally, We found that the splicing factors ILF2 and HNRNPA1 are highly co-expressed with DAS genes, suggesting their regulatory role in alternative splicing during RB progression. Further research is essential to confirm these findings and explore their potential in developing novel treatments for retinoblastoma.

Author Contribution Statement

Mohamed Hameed Aslam: Formal analysis, Writing-Original draft preparation, Bharanidharan Devarajan: Conceptualization, Reviewing and Editing, Vanniarajan Ayyasamy: Reviewing and Editing, and Usha Kim: Reviewing and Editing. All the authors reviewed and accepted the final version of the manuscript.

Acknowledgements

We gratefully acknowledge the Indian Council for Medical Research (ICMR) for providing financial support through the Senior Research Fellowship awarded to Mohamed Hameed Aslam A (Fellowship No. 2021-12986/BMI/11(80)/2022, dated 08.07.2022).

Ethical Approval

No ethical approval was required for this study.

Funding

Senior Research Fellow -Indian Council of Medical Research (ICMR), India.

Declaration of Competing Interest

We declared that none of the authors has financial and personal competing interests.

Data Availability

The datasets generated during and analysed during the current study are available from the corresponding author on request.

References

1. Dimaras H, Corson TW, Cobrinik D, White A, Zhao J, Munier FL, et al. Retinoblastoma. Nat Rev Dis Primers. 2015;1(1):15021. https://doi.org/10.1038/nrdp.2015.21
2. Rushlow DE, Mol BM, Kennett JY, Yee S, Pajovic S, Thériault BL, et al. Characterisation of retinoblastomas without rb1 mutations: Genomic, gene expression, and clinical studies. Lancet Oncol. 2013;14(4):327-34. https://doi.org/10.1016/s1470-2045(13)70045-7.
3. Dimaras H, Khetan V, Halliday W, Orlic M, Prigoda NL, Piovesan B, et al. Loss of RB1 induces non-proliferative retinoma: increasing genomic instability correlates with progression to retinoblastoma. Hum Mol Genet. 2008;17(10):1363–72. https://doi.org/10.1093/hmg/ddn024
4. Francis JH, Richards AL, Mandelker DL, Berger MF, Walsh MF, Dunkel IJ, et al. Molecular Changes in Retinoblastoma beyond RB1: Findings from Next-Generation Sequencing. Cancers. 2021;13(1):149. https://doi.org/10.3390/cancers13010149
5. McEvoy J, Ulyanov A, Brennan R, Wu G, Pounds S, Zhang J, et al. Analysis of mdm2 and mdm4 single nucleotide polymorphisms, mrna splicing and protein expression in retinoblastoma. PLoS One. 2012;7(8):e42739. https://doi.org/10.1371/journal.pone.0042739.

6. Choy KW, Lee TC, Cheung KF, Fan DS, Lo KW, Beaverson KL, et al. Clinical implications of promoter hypermethylation in rassf1a and mgmt in retinoblastoma. Neoplasia. 2005;7(3):200-6. https://doi.org/10.1593/neo.04565.
7. Zhang J, Benavente CA, McEvoy J, Flores-Otero J, Ding L, Chen X, et al. A novel retinoblastoma therapy from genomic and epigenetic analyses. Nature. 2012;481(7381):329-34. https://doi.org/10.1038/nature10733.
8. Rathore S, Verma A, Ratna R, Marwa N, Ghiya Y, Honavar SG, et al. Retinoblastoma: A review of the molecular basis of tumor development and its clinical correlation in shaping future targeted treatment strategies. Indian J Ophthalmol. 2023;71(7):2662-76. https://doi.org/10.4103/ijo.Ijo_3172_22.
9. Elchuri SV, Rajasekaran S, Miles WO. Rna-sequencing of primary retinoblastoma tumors provides new insights and challenges into tumor development. Front Genet. 2018;9:170. https://doi.org/10.3389/fgene.2018.00170.
10. Oltean S, Bates DO. Hallmarks of alternative splicing in cancer. Oncogene. 2014;33(46):5311–8. ttps://doi.org/10.1038/onc.2013.533
11. Cygan KJ, Soemedi R, Rhine CL, Profeta A, Murphy EL, Murray MF, et al. Defective splicing of the rb1 transcript is the dominant cause of retinoblastomas. Hum Genet. 2017;136(9):1303-12. https://doi.org/10.1007/s00439-017-1833-4.
12. Venkataramany AS, Schieffer KM, Lee K, Cottrell CE, Wang PY, Mardis ER, et al. Alternative rna splicing defects in pediatric cancers: New insights in tumorigenesis and potential therapeutic vulnerabilities. Ann oncol. 2022;33(6):578-92. https://doi.org/10.1016/j.annonc.2022.03.011.
13. Yang Z, Wang J, Zhu R. Identification of driver genes with aberrantly alternative splicing events in pediatric patients with retinoblastoma. Math Biosci Eng. 2020;18(1):328-38. https://doi.org/10.3934/mbe.2021017.
14. Chen S, Zhou Y, Chen Y, Gu J. Fastp: An ultra-fast all-in-one fastq preprocessor. Bioinformatics. 2018;34(17):i884-i90. https://doi.org/10.1093/bioinformatics/bty560.
15. Dobin A, Davis CA, Schlesinger F, Drenkow J, Zaleski C, Jha S, et al. Star: Ultrafast universal rna-seq aligner. Bioinformatics. 2013;29(1):15-21. https://doi.org/10.1093/bioinformatics/bts635.
16. Liao Y, Smyth GK, Shi W. Featurecounts: An efficient general purpose program for assigning sequence reads to genomic features. Bioinformatics. 2014;30(7):923-30. https://doi.org/10.1093/bioinformatics/btt656.
17. Robinson MD, McCarthy DJ, Smyth GK. Edger: A bioconductor package for differential expression analysis of digital gene expression data. Bioinformatics. 2010;26(1):139-40. https://doi.org/10.1093/bioinformatics/btp616.
18. Park JW, Tokheim C, Shen S, Xing Y. Identifying differential alternative splicing events from rna sequencing data using rnaseq-mats. Methods Mol Biol. 2013;1038:171-9. https://doi.org/10.1007/978-1-62703-514-9_10.
19. Wu T, Hu E, Xu S, Chen M, Guo P, Dai Z, et al. Clusterprofiler 4.0: A universal enrichment tool for interpreting omics data. Innovation (Camb). 2021;2(3):100141. https://doi.org/10.1016/j.xinn.2021.100141.
20. Shannon P, Markiel A, Ozier O, Baliga NS, Wang JT, Ramage D, et al. Cytoscape: a software environment for integrated models of biomolecular interaction networks. Genome Res. 2003;13(11):2498–504. https://doi.org/10.1101/gr.1239303
21. Langfelder P, Horvath S. WGCNA: an R package for weighted correlation network analysis. BMC Bioinformatics. 2008;9:559. https://doi.org/10.1186/1471-2105-9-559
22. Stelzer G, Plaschkes I, Oz-Levi D, Alkelai A, Olender T, Zimmerman S, et al. Varelect: The phenotype-based variation prioritizer of the genecards suite. BMC Genomics. 2016;17 Suppl 2(Suppl 2):444. https://doi.org/10.1186/s12864-016-2722-2.
23.Urbanski L, Brugiolo M, Park SH, Angarola BL, Leclair NK, Yurieva M, et al. MYC regulates a pan-cancer network of co-expressed oncogenic splicing factors. Cell Rep. 2022;41(8):111704. https://doi.org/10.1016/j.celrep.2022.111704
24. Schulze A, Oshi M, Endo I, Takabe K. MYC Targets Scores Are Associated with Cancer Aggressiveness and Poor Survival in ER-Positive Primary and Metastatic Breast Cancer. Int J Mol Sci. 2020;21(21):1–13. https://doi.org/10.3390/ijms21218127
25. Phillips JW, Pan Y, Tsai BL, Xie Z, Demirdjian L, Xiao W, et al. Pathway-guided analysis identifies Myc-dependent alternative pre-mRNA splicing in aggressive prostate cancers. Proc Natl Acad Sci U S A . 2020;117(10):5269–79. https://doi.org/10.1073/pnas.1915975117
26. De Vitis C, Battaglia AM, Pallocca M, Santamaria G, Mimmi MC, Sacco A, et al. ALDOC- and ENO2- driven glucose metabolism sustains 3D tumor spheroids growth regardless of nutrient environmental conditions: a multi-omics analysis. J Exp Clin Cancer Res. 2023;42(1):69. https://doi.org/10.1186/s13046-023-02641-0
27. Giacinti C, Giordano A. Rb and cell cycle progression. Oncogene. 2006;25(38):5220-7. https://doi.org/10.1038/sj.onc.1209615.
28. Warda O, Naeem Z, Roelofs KA, Sagoo MS, Reddy MA. Retinoblastoma and vision. Eye. 2023;37(5):797-808. https://doi.org/10.1038/s41433-021-01845-y.
29. Wang C, Zong X, Wu F, Leung RWT, Hu Y, Qin J. DNA- and RNA-Binding Proteins Linked Transcriptional Control and Alternative Splicing Together in a Two-Layer Regulatory Network System of Chronic Myeloid Leukemia. Front Mol Biosci. 2022;9:920492. https://doi.org/10.3389/fmolb.2022.920492
30. Balaji S, Rao A, Saraswathi KK, Sethu Nagarajan R, Santhi R, Kim U, et al. Focused cancer pathway analysis revealed unique therapeutic targets in retinoblastoma. Med Oncol . 2024;41(7):168. https://doi.org/10.1007/s12032-024-02391-9
31. Jahankhani K, Ahangari F, Adcock IM, Mortaz E. Possible cancer-causing capacity of COVID-19: Is SARS-CoV-2 an oncogenic agent? Biochimie. 2023;213:130. https://doi.org/10.1016/j.biochi.2023.05.014
32. Takebayashi SI, Tanaka H, Hino S, Nakatsu Y, Igata T, Sakamoto A, et al. Retinoblastoma protein promotes oxidative phosphorylation through upregulation of glycolytic genes in oncogene-induced senescent cells. Aging Cell. 2015;14(4):689. https://doi.org/10.1111/acel.12351
33. Jordan-Sciutto KL, Dorsey R, Chalovich EM, Hammond RR, Achim CL. Expression Patterns of Retinoblastoma Protein in Parkinson Disease. J Neuropathol Exp Neurol. 2003;62(1):68–74. https://doi.org/10.1093/jnen/62.1.68
34. Gómez-Romero L, Alvarez-Suarez DE, Hernández-Lemus E, Ponce-Castañeda MV, Tovar H. The regulatory landscape of retinoblastoma: a pathway analysis perspective. R Soc Open Sci. 2022;9(5):220031. https://doi.org/10.1098/rsos.220031
35. Kaewkhaw R, Rojanaporn D. Retinoblastoma: Etiology, Modeling, and Treatment. Cancers. 2020;12:2304. https://doi.org/10.3390/cancers12082304
36. Cruz-Gálvez CC, Ordaz-Favila JC, Villar-Calvo VM, Cancino-Marentes ME, Bosch-Canto V. Retinoblastoma: Review and new insights. Front Oncol . 2022;12:963780. https://doi.org/10.3389/fonc.2022.963780
37. Caligiuri I, Toffoli G, Giordano A, Rizzolio F, Caligiuri I,

Toffoli G, et al. pRb controls Estrogen Receptor alpha protein stability and activity. Oncotarget. 2013;4:875–83. https://doi.org/10.18632/oncotarget.1036
38. Mäkelä JA, Toppari J. Retinoblastoma-E2F Transcription Factor Interplay Is Essential for Testicular Development and Male Fertility. Front Endocrinol (Lausanne). 2022;13:903684. https://doi.org/10.3389/fendo.2022.903684
39. Gu W, Schneider JW, Condorelli G, Kaushal S, Mahdavi V, Nadal-Ginard B. Interaction of myogenic factors and the retinoblastoma protein mediates muscle cell commitment and differentiation. Cell. 1993;72(3):309–24. https://doi.org/10.1016/0092-8674(93)90110-c
41. Rajabi HN, Takahashi C, Ewen ME. Retinoblastoma Protein and MyoD Function Together to Effect the Repression of Fra-1 and in Turn Cyclin D1 during Terminal Cell Cycle Arrest Associated with Myogenesis. J Biol Chem. 2014;289(34):23417. https://doi.org/10.1074/jbc.M113.532572
41. Currie E, Schulze A, Zechner R, Walther TC, Farese R V. Cellular fatty acid metabolism and cancer. Cell Metab. 2013;18(2):153–61. https://doi.org/10.1016/j.cmet.2013.05.017
42. Hanahan D, Weinberg RA. Hallmarks of cancer: the next generation. Cell. 2011;144(5):646–74. https://doi.org/10.1016/j.cell.2011.02.013
43. Heiden MGV, Cantley LC, Thompson CB. Understanding the Warburg effect: the metabolic requirements of cell proliferation. Science. 2009;324(5930):1029–33. https://doi.org/10.1126/science.1160809
44. Kamphorst JJ, Cross JR, Fan J, De Stanchina E, Mathew R, White EP, et al. Hypoxic and Ras-transformed cells support growth by scavenging unsaturated fatty acids from lysophospholipids. Proc Natl Acad Sci U S A. 2013;110(22):8882–7. https://doi.org/10.1073/pnas.1307237110
45. Hensley CT, Faubert B, Yuan Q, Lev-Cohain N, Jin E, Kim J, et al. Metabolic Heterogeneity in Human Lung Tumors. Cell. 2016;164(4):681–94. https://doi.org/10.1016/j.cell.2015.12.034
46. Ge Y, He Z, Xiang Y, Wang D, Yang Y, Qiu J, et al. The identification of key genes in nasopharyngeal carcinoma by bioinformatics analysis of high-throughput data. Mol Biol Rep. 2019;46(3):2829–40. https://doi.org/10.1007/s11033-019-04729-3
47. Li Y, Li L, Zhao H, Gao X, Li S. Identifying Obstructive Sleep Apnea Syndrome-Associated Genes and Pathways through Weighted Gene Coexpression Network Analysis. Comput Math Methods Med. 2022;2022:3993509. https://doi.org/10.1155/2022/3993509
48. Terrones M, Op de Beeck K, Van Camp G, Vandeweyer G, Mateiu L. Transcriptomic analysis of ROS1+ non-small cell lung cancer reveals an upregulation of nucleotide synthesis and cell adhesion pathways. Front Oncol. 2024;14:1408697. https://doi.org/10.3389/fonc.2024.1408697
49. Nakajima R, Deguchi R, Komori H, Zhao L, Zhou Y, Shirasawa M, et al. The *TFDP1* gene coding for DP1, the heterodimeric partner of the transcription factor E2F, is a target of deregulated E2F. Biochem Biophys Res Commun. 2023;663:154–62. https://doi.org/10.1016/j.bbrc.2023.04.092
50. Ormondroyd E, De La Luna S, La Thangue NB. A new member of the DP family, DP-3, with distinct protein products suggests a regulatory role for alternative splicing in the cell cycle transcription factor DRTF1/E2F. Oncogene. 1995;11(8):1437–46.
51. Marković L, Bukovac A, Varošanec AM, Šlaus N, Pećina-Šlaus N. Genetics in ophthalmology: molecular blueprints of retinoblastoma. Hum Genomics. 2023;17(1):82. https://doi.org/10.1186/s40246-023-00529-w
52. Lu X, Lv XD, Ren YH, Yang WD, Li ZB, Zhang L, et al. Dysregulation of *TFDP1* and of the cell cycle pathway in high-grade glioblastoma multiforme: a bioinformatic analysis. Genet Mol Res. 2016;15(2). https://doi.org/10.4238/gmr.15027646
53. Wang L, Kong W, Liu B, Zhang X. Proliferating cell nuclear antigen promotes cell proliferation and tumorigenesis by up-regulating STAT3 in non-small cell lung cancer. Biomed Pharmacother. 2018;104:595–602. https://doi.org/10.1016/j.biopha.2018.05.071
54. Villegas-Ruíz V, Romo-Mancillas A, Medina-Vera I, Castro-López KA, Ramirez-Chiquito JC, Fonseca-Montaño MA, et al. The Proliferating Cell Nuclear Antigen (*PCNA*) Transcript Variants as Potential Relapse Markers in B-Cell Acute Lymphoblastic Leukemia. Cells. 2022;11(20):3205. https://doi.org/10.3390/cells11203205.
55. Sever-Chroneos Z, Angus SP, Fribourg AF, Wan H, Todorov I, Knudsen KE, et al. Retinoblastoma Tumor Suppressor Protein Signals through Inhibition of Cyclin-Dependent Kinase 2 Activity To Disrupt *PCNA* Function in S Phase. Mol Cell Biol. 2001;21(12):4032. https://doi.org/10.1128/MCB.21.12.4032-4045.2001
56. Chen Q, Ouyang L, Liu Q. Cyclin B1: A potential prognostic and immunological biomarker in pan-cancer. Biomol Biomed. 2024;24(5):1150-69. https://doi.org/10.17305/bb.2024.10253
57. Dominguez D, Tsai YH, Weatheritt R, Wang Y, Blencowe BJ, Wang Z. An extensive program of periodic alternative splicing linked to cell cycle progression. Elife. 2016;5:e10288. https://doi.org/10.7554/eLife.10288.
58. Li Y, Wang M, Yang M, Xiao Y, Jian Y, Shi D, et al. Nicotine-induced ilf2 facilitates nuclear mrna export of pluripotency factors to promote stemness and chemoresistance in human esophageal cancer. Cancer Res. 2021;81(13):3525–38. https://doi.org/10.1158/0008-5472.CAN-20-4160
59. Lee Y, Rio DC. Mechanisms and regulation of alternative Pre-mRNA splicing. Annu Rev Biochem. 2015;84:291–323. https://doi.org/10.1146/annurev-biochem-060614-034316
60. Das S, Krainer AR. Emerging Functions of SRSF1, Splicing Factor and Oncoprotein, in RNA Metabolism and Cancer. Molecular Cancer Res. 2014;12:1195–204. https://doi.org/10.1158/1541-7786.mcr-14-0131
61. Xiao Y, Cai G, Feng X, Li Y, Guo W, Guo Q, et al. Splicing factor YBX1 regulates bone marrow stromal cell fate during aging . EMBO J. 2023;42(9):e111762. https://doi.org/10.15252/embj.2022111762
62. Jaworska AM, Wlodarczyk NA, Mackiewicz A, Czerwinska P. The role of TRIM family proteins in the regulation of cancer stem cell self-renewal. Stem Cells. 2020;38:165–73. https://doi.org/10.1002/stem.3109
63. Lo A, McSharry M, Berger AH. Oncogenic KRAS alters splicing factor phosphorylation and alternative splicing in lung cancer. BMC Cancer. 2022;22:1–13. https://doi.org/10.1186/s12885-022-10311-1
64. Li J, Feng D, Gao C, Zhang Y, Xu J, Wu M, et al. Isoforms S and L of MRPL33 from alternative splicing have isoform-specific roles in the chemoresponse to epirubicin in gastric cancer cells via the PI3K/AKT signaling pathway. Int J Oncol. 2019;54(5):1591–600. https://doi.org/10.3892/ijo.2019.4728
65. Chen B, Piel WH, Gui L, Bruford E, Monteiro A. The HSP90 family of genes in the human genome: Insights into their divergence and evolution. Genomics. 2005;86(6):627–37. https://doi.org/10.1016/j.ygeno.2005.08.012
66. Cloutier P, Poitras C, Durand M, Hekmat O, Fiola-Masson

É, Bouchard A, et al. R2TP/Prefoldin-like component RUVBL1/RUVBL2 directly interacts with ZNHIT2 to regulate assembly of U5 small nuclear ribonucleoprotein. Nat Commun. 2017;8:15615 . https://doi.org/10.1038/ncomms15615